In Vivo Early Detection of Acute Radiation Dermatitis Using Optical Coherence Tomography (OCT) Images

Christos Photiou[1], Iosif Strouthos[2], Constantina Cloconi[2]

[1] KIOS Research and Innovation Center of Excellence, Dep of Electrical and Computer Engineering, University of Cyprus, 1 Panepistimiou Av., Nicosia, Cyprus, 1678

[2] Department of Radiation Oncology, German Oncology Center, 1 Nikis Avenue, Agios Athanasios, Limassol, Cyprus, 4108

ABSTRACT

Radiation therapy remains an essential component of cancer treatment, with nearly 50% of cancer patients receiving radiation therapy at some point during the course of their illness. Of those, as many as 90-95% may experience some form of acute radiation dermatitis (ARD) or radiation-induced skin injury. ARD results in significant discomfort, restriction of daily activities, overall decrease in the quality of life and even cessation of the necessary radiation therapy with detrimental survival effects. Unfortunately, research into the causes and possible management strategies for ARD is hindered by the lack of biomarkers for the quantitative assessment of the early changes associated with the condition. This study provides the basis to yield such novel biomarkers using Optical Coherence Tomography (OCT) images with the extraction of conventional image intensity and novel features. Patients were imaged twice each week over the six-week course of their radiation treatment. The severity of the cases was graded by an expert oncologist. Preliminary results, separating normal skin from early ARD, were very promising, yielding an accuracy of 88.3%.

1. INTRODUCTION

Acute radiation dermatitis (ARD) is a disease that appears in the majority of cancer patients as a side effect of radiation therapy. The complaints vary from erythema to moist or dry desquamation, which result in significant discomfort, restriction of daily activities, overall decrease in the quality of life (QoL) and even cessation of the necessary radiotherapy with detrimental effects [1,2]. Despite various studies reporting prevention or treatment of ARD, as well as guidelines published in 2013 [3], there is no standard therapy or consensus on the optimal management of the condition. Research into the causes and possible management strategies for ARD is further hindered by the lack of biomarkers for the quantitative assessment of the early changes associated with the condition. OCT is well suited for the evaluation of ARD since it can perform imaging at a resolution approaching that of histopathology (~10 μm) in real-time, does not require any contact with the patient's already-injured skin and its penetration depth (~ 2 mm) allows the visualization of the skin's diagnostically important layers such as the epidermis and top layer of the dermis. In dermatology, researchers have investigated the diagnostic ability of OCT, *in vivo*, for the evaluation of basal cell carcinomas, psoriasis, allergic dermatitis and detection of radiation effects on mouse skin [4-7]. In all cases, the sensitivity and specificity reached the ranges of 80% to 96%. However, even skilled observers find it very challenging to evaluate OCT images by visual inspection alone [8]. To alleviate this problem, studies attempted to extract various features from OCT images, including intensity- and texture- based features [9]. Recently our team extracted features from the OCT data leading to biomarkers correlating to tissue abnormalities. These novel features include group velocity dispersion, scatterer size (corresponding mainly to cell nucleus size) and index of refraction which are affected by and reflect biochemical changes of disease [10-14]. In this study, *in vivo* head and neck OCT images, from patients undergoing radiation therapy, were collected during the course of their treatment and evaluated using a fully automated algorithm for image segmentation and feature extraction. Machine learning classifiers were utilized to differentiate normal skin from early ARD.

2. METHODOLOGY

A. Image and Data Processing

The OCT images were collected using a swept source OCT system with a center wavelength of 1300 nm, an axial resolution of 10 μm and an A-Scan rate of 40 kHz. The study was performed at the German Oncology Center (GOC), Limassol, Cyprus. For this first proof-of-concept, six male and female volunteers (>18 years old) with head and neck cancers scheduled to undergo radiation therapy at the GOC were enrolled after bioethics approval. Exclusion criteria include

patients with disabilities, pregnant women, patients with prior radiation therapy at the area of examination (last six months), children, and patients with autoimmune diseases. After informed consent, a predefined area at the irradiated side of the neck of the subjects, was imaged with OCT. Six images were acquired, every 1 cm, to cover the region from the mandibular angle to the clavicle. A photograph of the same area was also taken with a digital camera. The imaging was repeated prior to every radiation therapy session, twice per week, for the duration of the six-week therapy, resulting in a dataset of 438 images. During each visit, the patient's ARD grade, at the same six positions imaged, was noted.

B. Feature Extraction

Automated algorithms were developed to segment the images, into epidermis and dermis layers, and extract image features from the OCT images of all patients. The features included: (i) *First order intensity statistics:* Various first order statistical features of the intensity distribution extracted from predefined neighborhoods of each image including the mean, standard deviation, variance, skewness, median, kurtosis, min, max; (ii) *Gray Level Co-occurrence Matrix (GLCM):* The four main features of the GLCM, which quantitatively describe perceptual texture properties, calculated: Correlation, contrast, homogeneity and energy; (iii) *Novel feature – Group Velocity Dispersion (GVD):* Measurement of the GVD *in vivo* performed using the speckle degradation method [14]. Changes in dispersion, a measure of the variation of the index of refraction of a material as a function of the wavelength of light, can be indicative of biochemical variations caused by the disease; and (iv) *Novel feature – Scatterer Size (SS)*: The mean SS estimated using Mie Theory and the bandwidth of the correlation of the derivative (COD) of the OCT spectrum, obtained from a frequency transformation [12]. For each extracted feature, its statistics over the entire image were calculated (mean, median, variance, standard deviation, kurtosis, skewness, sum, minimum, maximum) resulting in 1268 features for every image.

C. Feature Selection and Classification

Feature selection and optimization was performed in an effort to choose the features that result in the best classification accuracy and can act as possible early ARD biomarkers. This process began with a chi-square test to rank features in order of significance. Prior to the classification, the final dataset, which included the most significant features, was normalized. Due to the fact that the dataset was imbalanced, Synthetic Minority Oversampling Technique (SMOTE) was utilized to increase the data points and avoid overfitting issues that can occur due to a minority class. A Linear Discriminant Analysis (LDA) classifier was utilized since it provided the best accuracy compared to other classifiers. The performance was verified using leave-one-patient-out cross-validation, to avoid introducing any bias to the results.

3. EXPERIMENTAL RESULTS

Figure 1 shows an example of *in vivo* head and neck OCT images from the same patient acquired at three different time points during radiation therapy. The algorithm automatically marked the top surface of the tissue and its two layers, the epidermis and dermis (Fig. 1, green lines). Fig. 1A is an image acquired prior to any therapy representing normal skin. An image of the same region acquired on week 4 of the therapy is shown in Fig. 1B (grade 1) while Fig. 1C was acquired during week 6 (grade 2a). The segmented epidermis and dermis of the annotated region are also shown in Fig.1, illustrating how challenging it would be to classify each by visual inspection alone.

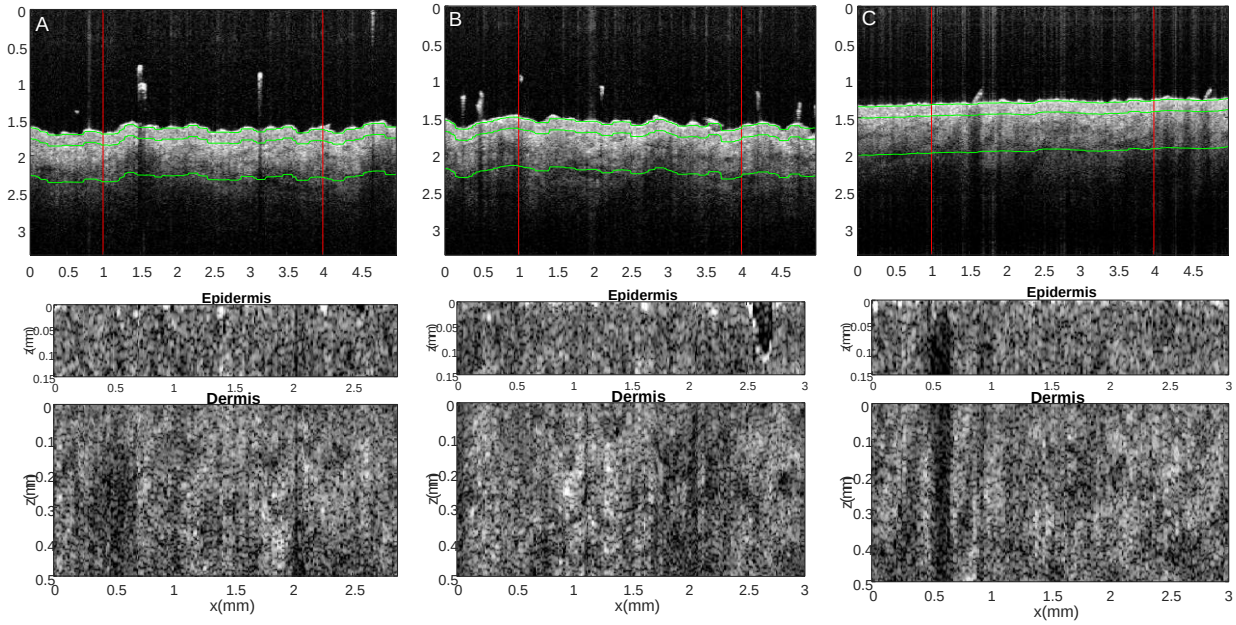

Figure 1. (A) *In vivo* head and neck OCT image before the first week of radiation therapy. The region between the red vertical lines was used for the classification. Below are the two layers of the segmented regions, the epidermis and dermis, used for feature extraction. (B) Image of the same area in the same patient, during the fourth week and (C) during the sixth week of radiation therapy.

The regions of the epidermis and dermis of each image were used to extract the features described above. The window size was 202 x 11 pixels (0.15 x 0.11 mm) for the epidermis region and 336 x 11 pixels (0.25 x 0.11 mm) for the dermis region. Fourteen first and second order intensity statistics of the epidermis along with the GVD and SS from the dermis appeared to be the most significant for the classification.

A Linear Discriminant Analysis (LDA) classifier was utilized for normal vs early ARD classification, showing very promising results with a sensitivity of 91.8%, specificity of 75% and accuracy of 88.3%. The classification performance was verified using a leave-one-patient-out-cross validation approach. MANOVA was performed, to optimally separate the two classes, only for the visualization of the results (Figure 2).

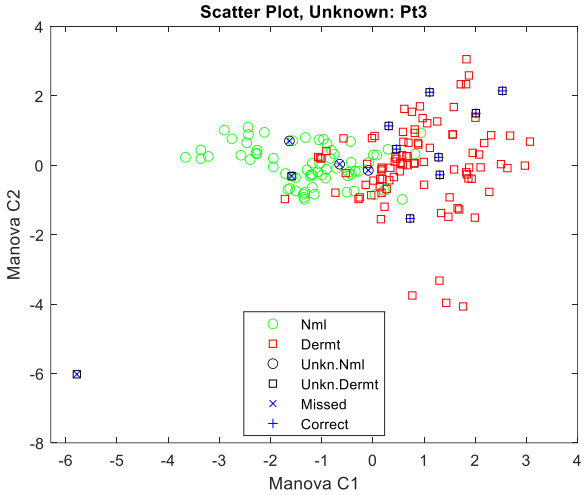

Figure 2. MANOVA scatter plot displaying the classification results using LDA and leave-one-patient-out-cross-validation. Green circles and red squares are the normal and ARD training data points respectively. Blue circles and squares indicate the data points from the unknown patient. Marked with a cross (+) are the correctly classified points, whereas marked with an x are the misclassified ones.

4. CONCLUSIONS

Given the preliminary results presented in this study, the automated algorithm proposed could be further developed to perform *in vivo* early detection and classification of ARD in patients undergoing radiation therapy. Using machine learning with LDA, the algorithm could distinguish normal skin tissue from early ARD with an accuracy of 88.3%, sensitivity of 91.8% and specificity of 75%. Although, these results are very promising, further evaluation is required, with a larger number of images from more patients, in order to optimize the segmentation and classifier models and, also, introduce deep learning. This work has the potential to be developed into a system that can be used for effective computer aided diagnosis of ARD at the early stage that could help guide both the management of the disease but, also, much-needed future research and significantly impact patient prognosis and quality of life.

Acknowledgments

This study is funded by the European Union's Horizon 2020 research and innovation programme under grant agreement No 739551 (KIOS CoE) and from the Republic of Cyprus through the Directorate General for European Programmes, Coordination and Development.

5. REFERENCES

1. Singh M, Afsaneh A., Rebecca W., and Sadanori A., "RD: A Review of Our Current Understanding." 17:277 (2016)
2. Lopez E, Isabel N, Rosario G, Rosario M, Juan, Rodríguez M, Teresa V, Mercedes V, and Jose A, "Breast Cancer Acute Radiotherapy Morbidity Evaluated by Different Scoring Systems," 73:127 (2002)
3. Wong RK, Bensadoun RJ, Boers CB, Bryce J, Chan A, Epstein JB, Eaby B, Lacouture ME, "Clinical practice guidelines for the prevention and treatment of acute radiation reactions from the MASCC Group," 21:2933-48 (2013)
4. Hussain AA, Themstrup L, Jemec GB, "Optical coherence tomography in the diagnosis of basal cell carcinoma," 307:1-10 (2015)
5. Morsy H, Kamp S, Thrane L, Behrendt N, Saunder B, Zayan H, Elmagid EA, Jemec GB, "OCT imaging of psoriasis vulgaris: correlation with histology and disease severity," 302:105-111 (2010)
6. Boone MA, Jemec GB, Del Marmol V, "Differentiating allergic and irritant contact dermatitis by high-definition OCT: a pilot study," 307:11-22 (2015)
7. Lee J, Jang WH, Shim S, Kim B, Jang WS, Myung JK, Park S, Kim KH, "Characterization of early-stage cutaneous radiation injury by using optical coherence tomography angiography," 11:2652-64 (2020)
8. Holmes JV, von Braunmühl T, Berking C, Sattler E, Ulrich M, Reinhold U, Kurzen H, Dirschka T, Kellner C, Schuh S, Welzel J, "OCT of BCC: influence of location and subtype on diagnostic performance," Brit J Dermatol, 178:1102-10 (2018)
9. Gao W, Valery PZ, Oleg OM, Ivan AB, Dmitry NA and Dmitry VK, Medical images classification for skin cancer using quantitative image features with OCT," Optic Health Sci, 9:1650003 (2016)
10. Photiou C. and Pitris C., "Comparison of tissue dispersion measurement techniques based on OCT," J. Biomed. Opt. 24(4), 046003 (2019)
11. Photiou C, Bousi E, Zouvani I. and Pitris C, "Using speckle to measure tissue dispersion in optical coherence tomography", Biomed. Opt. Express 8, 2528-2535 (2017)
12. Kassinopoulos M, Bousi E, Zouvani, I. and Pitris C, "Correlation of the derivative as a robust estimator of scatterer size in OCT", Biomed. Opt. Express 8, 1598-1606 (2017)
13. Photiou C. and Pitris C, "Dual-angle OCT for index of refraction estimation using rigid registration and cross-correlation," J.Opt. 24(10), 106001 (2019)
14. Photiou C, Plastiras G. and Pitris C, "ML Methods for Barret's and Dysplasia classification from In Vivo OCT Images of Human Esophagus,"OSA paper OW2E (2020)